TÜBİTAK

Turkish Journal of Chemistry

http://journals.tubitak.gov.tr/chem/

Research Article

Turk J Chem
(2018) 42: 572 – 585

doi:10.3906/kim-1707-54

Synthesis of quaternized zinc(II) and cobalt(II) phthalocyanines bearing pyridine-2-yl-ethynyl groups and their DNA binding properties

Maryam MOEINI ALISHAH, Hacer Yasemin YENİLMEZ, İbrahim ÖZÇEŞMECİ, Behice Şebnem SESALAN, Zehra ALTUNTAŞ BAYIR*

Department of Chemistry, Faculty of Science and Letters, İstanbul Technical University, İstanbul, Turkey

Received: 21.07.2017 • **Accepted/Published Online:** 12.01.2018 • **Final Version:** 27.04.2018

Abstract: The synthesis and biological properties of tetra-substituted zinc and cobalt phthalocyanines bearing ethynylpyridine units on the periphery and their quaternized derivatives have been reported. The binding of quaternized ZnPc and CoPc (Q-ZnPc and Q-CoPc) with calf thymus DNA was investigated by UV-Vis spectrophotometric methods and thermodynamics. The mixtures of Q-ZnPc or Q-CoPc and DNA solutions were used to determine the change in the thermal melting temperature of DNA with the thermal denaturation profile. Thermodynamic parameters that show the spontaneity of the reactions between DNA and the quaternized phthalocyanines were investigated. K_b binding constants at a degree of 10^5 and 10^6 for Q-ZnPc and Q-CoPc, respectively, showed that the phthalocyanines bound to DNA fragments efficiently and thermodynamic data proved that the binding process was spontaneous and entropy-driven. The interactions between Q-ZnPc and Q-CoPc and DNA in an aqueous environment corresponded to electrostatic attractions and nonspecific binding.

Key words: Phthalocyanine, pyridine, calf thymus DNA, cross-coupling, entropy

1. Introduction

Phthalocyanines (Pcs), being tetrapyrrolic macrocycle derivatives, constitute an important class of compounds both in basic research and in applied sciences.[1] Adding desired functional groups to the periphery of Pc rings changes their optical, electronic, and catalytic properties and enables them to be used in different areas.[2] Owing to these properties, phthalocyanines have been used in dyestuffs, photochromic and electrochromic materials, liquid crystals, catalysts, chemical sensors, gas sensors in the form of Langmuir–Blodgett films, and nonlinear optical materials.[3–5]

Adding water-soluble groups to phthalocyanines as functional groups has also enabled them to be studied in the therapy of cancer. Today, Pcs are being used as second-generation photosensitizers. Compared with first-generation photosensitizers such as hematoporphyrin derivative, metallophthalocyanines (MPcs) have a much higher extinction coefficient of the Q band near 680 nm, which means that they are efficiently excited directly through tissue, whereas the introduction of hydrophilic groups into substituted Pc derivatives has been performed in order to achieve solubility in aqueous media. Pcs having water-soluble groups have a strong influence on the bioavailability and in vivo distribution, while the ionic groups provide binding of Pcs to DNA and proteins (e.g., BSA).

*Correspondence: bayir@itu.edu.tr

The interactions of cationic dyes with synthetic and natural DNAs have been widely researched.[6] Considering the mechanism of interactions may contribute to the design of more efficient drugs that target DNA. While the cationic porphyrins for DNA were employed for the treatment of cancer many years ago, the binding of cationic Pcs to DNA are much less developed.[7] The positively charged Pcs are one of the most efficient compounds to bind and cleave DNA of tumor cells.[8–10]

Metals are essential cell components in all living species as they are required in many biochemical reactions. They are also involved in a large number of functions, and metal proteins represent about 30% of all proteins.[11] The coordinated metal ions are important for the biological action of nucleic acids. It is believed that metal ions serve to screen the negative charges by direct interactions with the phosphate oxygen atoms [Co-DNA]. Transition metal ions such as cobalt(II), copper(II), and zinc(II) have different binding characteristics toward DNA.[11,12] For instance, cobalt is an interesting bioelement that dominates and interferes with many biological reactions. It was reported that, in crystals, the Co(II) ion binds exclusively at the N7 position of guanine bases by direct coordination.[12–14]

Carbon–carbon bond formation is the imperative stage for the synthesis of complicated organic structures. The formation of carbon–carbon, alkene, and alkyl bonds between Pc and the substituent attracts considerable attention because it enhances the aromaticity. Using this method, a number of Pcs have been synthesized with advanced catalytic, photophysical, and biological activities.[15,16] Previously we reported a procedure for the synthesis of carbon–carbon bonds between Pc and a substituent involving a Pd-catalyzed cross-coupling reaction.[17,18] Our previous studies also reported the biological efficacy of novel quaternized Pcs to assess their potential application in biology.[19–23] In this microscopic framework, the goal of this work is to synthesize novel tetra-substituted MPcs (Zn, Co) appending ethynylpyridine groups and their quaternized derivatives, which have potential use in biology. To clarify the binding mode of quaternized Pcs to calf thymus (CT) DNA, UV-Vis titration experiments and thermodynamics were employed.

2. Results and discussion

2.1. Synthesis of phthalocyanine derivatives

Substituted Pcs could be synthesized by two different methods. First, cyclotetramerization is carried out after the dinitrile derivative of the desired substituent is synthesized.[24] The second method is cyclotetramerization followed by the reaction of the desired groups with the ring.[25,26] In our previous study, we found that phthalocyanines bound by an ethynyl bridge have problems regarding purification. Therefore, we aimed to synthesize the desired phthalocyanines by the second method. First, tetraiodozinc and cobalt phthalocyanines were synthesized according to the literature (Scheme 1).[27] In the second part of the work, the bonding of the 2-ethynyl-pyridine group to the Pc ring was performed. Under typical Sonogashira reaction conditions, the cross-coupling reaction between an excess of 2-ethynylpyridine and tetraiodo-MPcs in triethylamine with copper(I) iodide (CuI) and bis(triphenylphosphine) palladium(II) chloride [$Pd(PPh_3)_2Cl_2$] as catalysts at room temperature under nitrogen atmosphere produced compounds **3** and **4** (Scheme 2). Pyridylethynyl-substituted Pc derivatives were separated from the starting materials by washing with methanol and acetone. For the synthesis of water-soluble Pc derivatives, pyridine groups were introduced into the reaction to synthesize quaternized derivatives.[9] The Pcs were reacted with an excess amount of dimethyl sulfate in DMF at 120 °C (Scheme 2). The reaction product was purified by washing with ethanol, ethyl acetate, THF, chloroform, and diethyl ether, respectively. Thus, water-soluble pyridine-substituted Pc derivatives were synthesized. All compounds are soluble in DMF and DMSO.

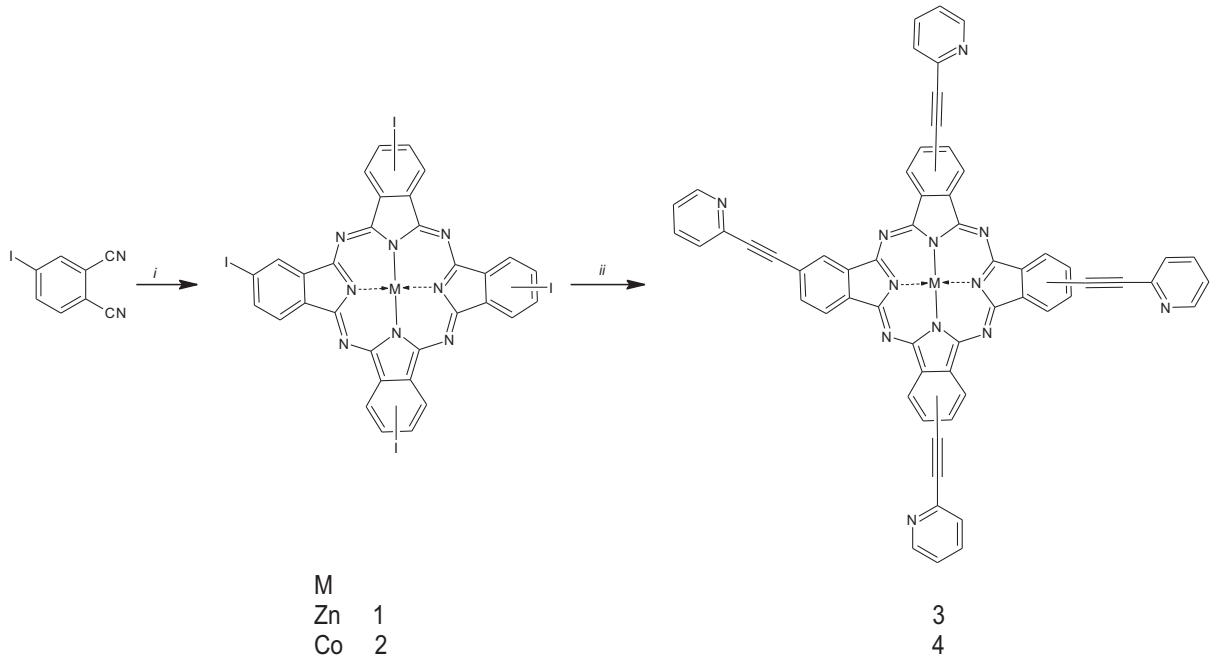

Scheme 1. Synthesis of 2, 9 (10), 16 (17), 23 (24)-tetra-(2-pyridylethynyl) metallophthalocyanines **3** and **4** (i: metal salt, 2-dimethylaminoethanol under N_2; ii: 2-ethynylpyridine, $Pd(PPh_3)_2Cl_2$, CuI, triethylamine under N_2).

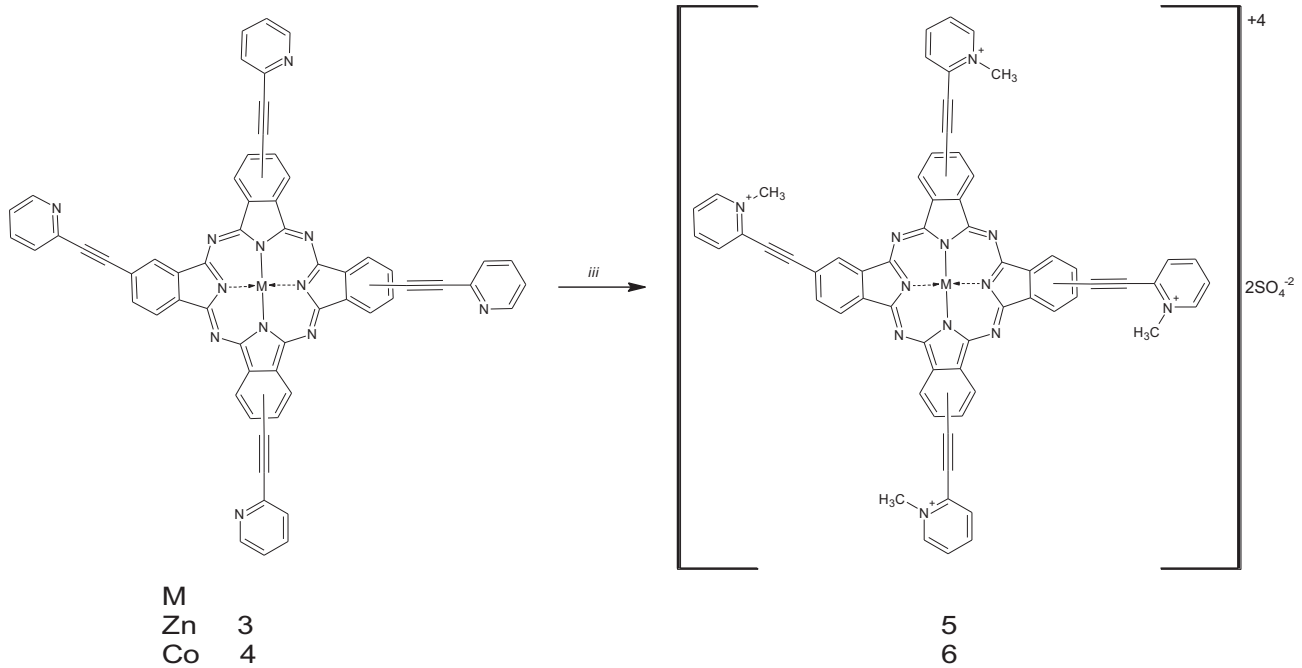

Scheme 2. Synthesis of quaternized metallophthalocyanines **5** and **6** (iii: dimethy lsulfate, DMF, 120 °C).

Spectral data (^{1}H NMR, UV-Vis, and FT-IR) for all new products are consistent with the proposed structures. In the NMR spectrum of compound **3**, peaks belonging to pyridine groups were observed in the

range of 7.46–7.61 ppm and protons on the Pc ring were observed in the range of 8.34–9.11 ppm. The NMR spectra of both compounds support the formation of the compound.

The FT-IR spectra of the Pcs **3** and **4** are very similar. In the FT-IR spectra of compounds **3** and **4**, stretching vibrations of C ≡ C groups are observed at 2209 cm^{-1} and 2207 cm^{-1}, respectively. The aromatic groups appeared at 3057–3060 cm^{-1} and the aromatic C – H bending vibrations were observed at 1597–1468 cm^{-1} at expected frequencies. The FT-IR spectra of the quaternized Pcs are very similar to their Pcs. No major change was found in the FT-IR spectra of **5** and **6** after quaternization. However, stretching vibrations were observed around 1385–1395 and 738–743 cm^{-1} for S = O and S - bonds, respectively.

By the definition of Pcs, their UV-Vis spectra have a distinguishing property. The transition between $\pi - \pi^*$ displays 2 separate bands, a Q-band in the region of 600–700 nm and a B-band in the 300–350 nm region.[28,29] The zinc Pcs (**3** and **5**) were observed around the Q-band of 681–679 and B-band of 357–334 nm in DMF. In the case of the cobalt Pc derivatives (**4** and **6**), Q-bands were observed around 664 while B-bands were observed at around 333 nm in DMF. These results show that the Pc ring was formed.

2.2. Aggregation properties of complexes 1–6

The aggregation behavior of Pcs is described as the coplanar association of rings progressing from monomers to dimers and to higher order complexes. It depends on the concentration, nature of the solvent, substituents, metal ions, and temperature.[30] The aggregative behavior of the Pcs (**1**–**6**) (Figures 1a–1c and 2a–2c) was examined at different concentrations in DMF. The intensity of absorption of the Q-band also increased with an increase in concentration. It was observed that a new band did not occur due to the aggregated species.[12] The Beer–Lambert law was obeyed for all these compounds for the concentrations ranging from 4.00×10^{-6} to 14.00×10^{-6} M in DMF. In order to verify this phenomenon, an aggregation study was performed in the presence of nonionic surfactant Triton-X. The results showed that no appreciable aggregations could be eliminated by the addition of Triton-X. Changes in the absorbance spectra are only those that correspond to the reduction of concentrations. By evaluating these studies, it can be concluded that the studied Pcs did not show aggregation in DMF at different concentrations.[17]

2.3. The evaluation of binding of Q-ZnPc and Q-CoPc with CT-DNA by UV-Vis titrations

Metal ion coordination to nucleic acids is not only required for charge neutralization; it is also essential for the biological function of nucleic acids. The structural impact of different metal ion coordinations on DNA helices is questionable.[14] The interactions may either be through direct metal ion coordination or mediated through water molecules of the metal ion's hydration shell. It is known that the interaction of purines and/or pyrimidines with chelating compounds destabilizes the nature of DNA.[31] As the interaction increases, the absorption of Q-ZnPc and Q-CoPc decreases and a more stable Pcs-DNA complex is formed. The last lines in Figures 3 and 4 were recorded on top of each other, after the last addition of DNA to the solutions of Q-ZnPc and Q-CoPc. The Q-band absorbances of Q-ZnPc and Q-CoPc remained constant, which means that stable Pc-DNA complexes were formed.

In Q-ZnPc, zinc could coordinate with oxygens and nitrogens in DNA bases.[32,33] The hypochromism suggested a close positioning of cationic Pcs to the DNA helix due to strong electrostatic interactions between the positively charged pyridinium groups and the phosphate backbone of DNA. According to Figure 3, the disappearance of absorption close to 679 nm is proved in Figure 5. The CT-DNA binding constant (K_b) of Q-ZnPc and Q-CoPc was found with the Wolfe–Shimer equation (Figure 5). Zinc(II) might be bound especially

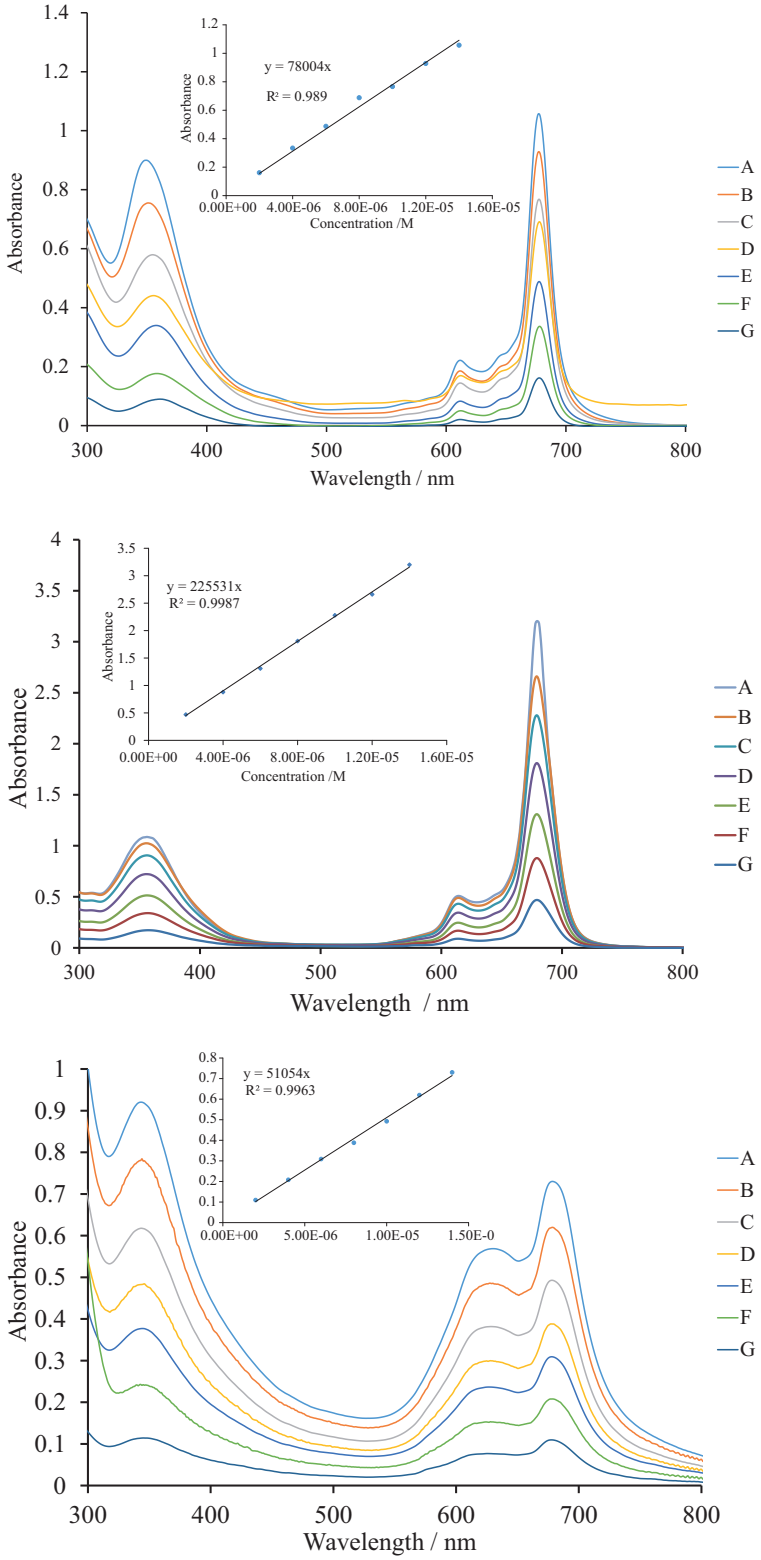

Figure 1. Aggregation behavior of zinc phthalocyanine derivatives (**1**, **3**, **5**) in DMF at different concentrations: 14 × 10^{-6} (A), 12 × 10^{-6} (B), 10 × 10^{-6} (C), 8 × 10^{-6} (D), 6 × 10^{-6} (E), 4 × 10^{-6} (F), and 2 × 10^{-6} (G) M.

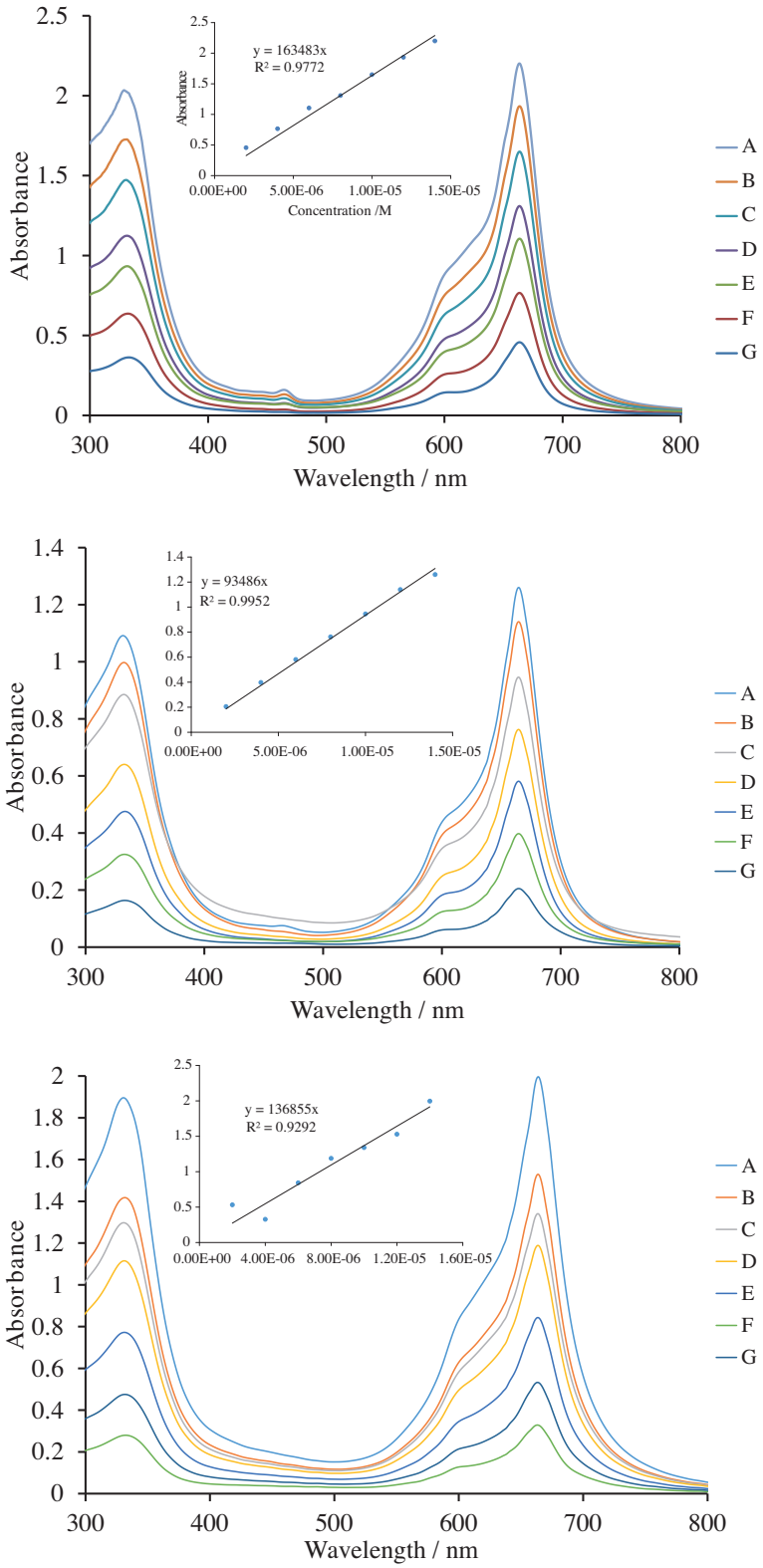

Figure 2. Aggregation behavior of cobalt phthalocyanine derivatives (**2**, **4**, **6**) in DMF at different concentrations: 14×10^{-6} (A), 12×10^{-6} (B), 10×10^{-6} (C), 8×10^{-6} (D), 6×10^{-6} (E), 4×10^{-6} (F), and 2×10^{-6} (G) M.

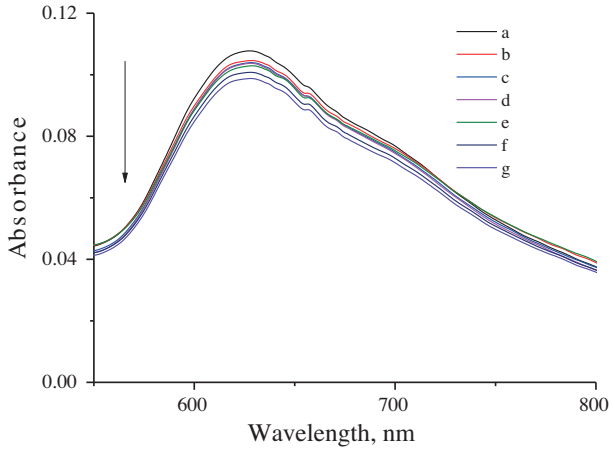

Figure 3. The spectral changes in UV-Vis absorption spectrum of Q-ZnPc (2.0×10^{-5} M) in buffer solution upon addition of DNA (5.0×10^{-5} M): a) 0 M; b) 4.95×10^{-7} M; c) 9.80×10^{-7} M; d) 1.46×10^{-6} M; e) 1.92×10^{-6} M; f) 2.38×10^{-6} M; g) 2.83×10^{-6} M.

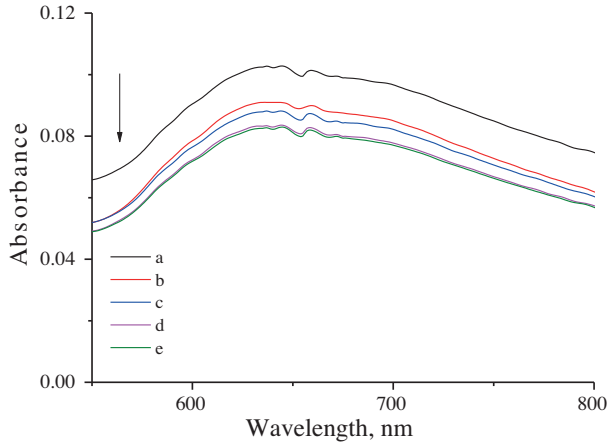

Figure 4. The spectral changes in UV-Vis absorption spectrum of Q-CoPc (2.0×10^{-5} M) in buffer solution upon addition of DNA (5.0×10^{-5} M): a) 0 M; b) 4.95×10^{-7} M; c) 9.80×10^{-7} M; d) 1.46×10^{-6} M; e) 1.92×10^{-6} M.

with N7 in guanines and oxygens in the phosphate skeleton to stabilize monomeric forms of Q-ZnPc. The K_b value supported that Q-ZnPc could bind to DNA electrostatically and nonspecifically (Figure 5; Table 1).[34] The K_b value of Q-CoPc, which is consistent with a stronger interaction than that of Q-ZnPc (Figure 4), could suggest the coordination of oxygens or nitrogens present in DNA stronger than in Q-ZnPc and also binding to phosphates electrostatically (Figures 4 and 5).[35] Generally high binding values could result due to the planar, rigid, and triply bonded pyridyl groups, which can intercalate with DNA easily.[36]

2.4. The evaluation of thermodynamic parameters

The data presented in Table 2 show that the favorable free energy changes of the binding process for Q-ZnPc and Q-CoPc arose from the large positive entropy changes. Entropy-driven binding processes took place according to thermodynamic parameters given in Table 2. When $\Delta H^\circ > 0$ and $\Delta S^\circ > 0$, the effective force is

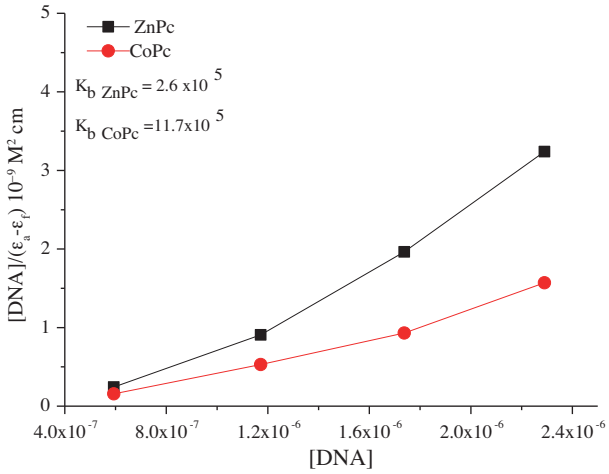

Figure 5. Wolfe–Shimer equation plot of CT-DNA binding constant (K_b) of Q-ZnPc and Q-CoPc.

Table 1. K_b binding constants of Q-ZnPc and Q-CoPc.

K_b ($\times 10^5$) (L mol^{-1})	
Q-ZnPc	2.6 ± 0.1
Q-CoPc	11.7 ± 0.1

hydrophobic.[37] The large positive entropic value was due to the removal of water from hydrophobic parts, resulting from aggregation in buffer solution.[38]

Table 2. Calculated thermodynamic parameters for binding of Q-ZnPc and Q-CoPc to ct-DNA (± STD).

T (K)	(LnK)	ΔG° (kJ mol^{-1})	ΔH° (kJ mol^{-1})	TΔS° (kJ mol^{-1} K^{-1})
Q-ZnPc				
293.15	6.21 ± 0.05	–15.48 ± 0.1	26.01 ± 0.1	41.49 ± 0.30
303.15	6.21 ± 0.05	–16.89 ± 0.1	26.01 ± 0.1	42.90 ± 0.30
313.15	7.14 ± 0.05	–18.31 ± 0.1	26.01 ± 0.1	44.32 ± 0.30
323.15	7.48 ± 0.05	–19.72 ± 0.1	26.01 ± 0.1	45.73 ± 0.30
333.15	7.73 ± 0.05	–21.14 ± 0.1	26.01 ± 0.1	47.15 ± 0.30
Q-CoPc				
293.15	12.01 ± 0.05	–28.25 ± 0.1	34.99 ± 0.1	63.22 ± 0.30
303.15	12.10 ± 0.05	–30.41 ± 0.1	34.99 ± 0.1	65.37 ± 0.30
313.15	12.36 ± 0.05	–32.56 ± 0.1	34.99 ± 0.1	67.53 ± 0.30
323.15	12.65 ± 0.05	–34.72 ± 0.1	34.99 ± 0.1	69.68 ± 0.30
333.15	12.99 ± 0.05	–36.88 ± 0.1	34.99 ± 0.1	71.84 ± 0.30

Incorporation of zinc had a great effect on the energetics of the binding process. At high temperature, more water molecules were released around the Q-ZnPc–DNA complex and entropy increased. Taking into account the UV-Vis spectra and K_b value, it can be said that Q-ZnPc and DNA could be nonspecific and electrostatically bonded to each other.

According to the thermodynamic parameters given in Table 2, the binding of Q-CoPc with DNA was also an entropy-driven process and the enhancement of water molecules around the DNA increased entropy. Thus, more negative Gibbs free energy was released during the interaction. The enlargement of entropy proved the formation of DNA–Q-CoPc or DNA–Q-ZnPc fragments. Water molecules around the DNA were displaced by cationic Pcs due to the electrostatic attraction forces between phosphates and quaternized pyridine groups.

When compared with Q-ZnPc, according to thermodynamic data and K_b binding values, Q-CoPc had stronger interaction with bases and phosphates of DNA. In the literature, it was reported that cobalt(III) Schiff-base complexes could selectively inhibit a zinc finger transcription factor.[39,40] In another previously reported work, ^{1}H NMR spectroscopy was used to confirm the structure of a zinc finger peptide that was disrupted by axial ligation of the cobalt(III) complex to the nitrogen of the imidazole ring of a histidine residue.[32]

2.5. The evaluation of the thermal denaturation profile of DNA

The DNA melting profile is very informative about the stability of the helix. The thermal melting temperature (T_m) of DNA is defined as the temperature at which half of the DNA strands are in the single-stranded DNA state.[41] The thermal denaturation profile is shown in Figure 6. Under the same set of conditions, in the presence of cationic Pcs, T_m values with standard deviations for Q-ZnPc and Q-CoPc were calculated as 55.4 $\pm$ 0.11 °C and 75.1 $\pm$ 0.11 °C, respectively. The T_m of DNA in the absence of any Pc was found to be 70 $\pm$ 1 °C. T_m is defined as the temperature at which half of the polynucleotide strand dissociates from double-stranded to single-stranded DNA.[39] Generally, the binding of metal complexes with DNA stabilizes the double helix structure. It is known that if the metal complexes stabilize the double-stranded DNA, the T_m of DNA will increase.[35,39,42] After the interaction of Q-CoPc with DNA, a high ΔT_m value could suggest that planar and triple-bonded pyridyl groups intercalate with bases of DNA.[39] Q-ZnPc destabilized double-stranded DNA caused dissociation at lower temperatures.[43]

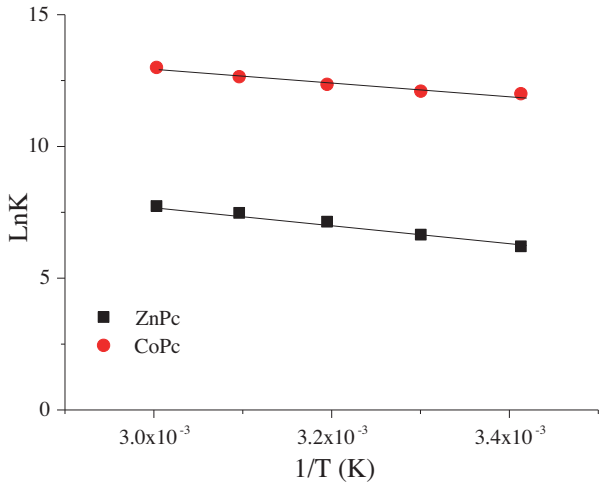

Figure 6. van't Hoff plots: temperature dependence of equilibrium constant for Q-ZnPc and Q-CoPc–DNA interactions.

2.6. Conclusions

In this study, ethynylpyridine-substituted Zn(II) and Co(II) phthalocyanines were synthesized and their water-soluble derivatives were prepared by quaternization. The structures of the new compounds were elucidated with

^{1}H NMR, FT-IR, and UV-Vis techniques. The aggregative behavior of the complexes was examined at different concentrations in DMF. According to our experimental results, both Q-CoPc and Q-ZnPc could bind to DNA efficiently with entropy-driven processes spontaneously. High binding constants and the thermodynamic data supported that, due to the electrostatic attractions and metal–DNA coordination, Q-ZnPc and Q-CoPc bind with DNA in a spontaneous and nonspecific manner. Q-CoPc and Q-ZnPc might coordinate with nitrogens, oxygens, or sulfurs. They also bind with phosphates of DNA in an electrostatic manner. To examine the mechanism of binding processes of Q-ZnPc and Q-CoPc with DNA, additional experiments and techniques that focus on the interactions of paramagnetic and diamagnetic metals with DNA should be employed.

3. Experimental

3.1. Materials and equipment

All the chemicals used in the synthesis were obtained from Sigma-Aldrich. Disodium salt of deoxyribonucleic acid from calf thymus was purchased from MP Biomedicals. Buffer solution (disodium hydrogen phosphate/potassium dihydrogen phosphate, pH 7) was purchased from Merck.

All reported ^{1}H NMR spectra were recorded on an Agilent VNMRS 500 MHz spectrometer. Chemical shifts (δ) were reported relative to Me_4Si as an internal standard. IR spectra were recorded on a PerkinElmer One FT-IR spectrophotometer and electronic spectra were recorded using a Scinco LabProPlus UV/Vis spectrophotometer with 1-cm path-length quartz cuvettes in the spectral range of 300–800 nm. Tetraiodozinc (**1**) and cobalt (**2**) phthalocyanines were synthesized according to the literature.[27]

3.2. The general route for the synthesis of 2-pyridylethynyl-substituted-phthalocyanines (3, 4)

Tetraiodo-phthalocyanine derivative (**1** or **2**) (100 mg, 0.093 mmol) was reacted with 2-ethynylpyridine (42 mg, 0.409 mmol) in the presence of bis(triphenylphosphine) palladium(II) chloride [$Pd(PPh_3)_2Cl_2$] (5 mg, 0.007 mmol) and copper(I) iodide (5 mg, 0.026 mmol) in 2 mL of triethylamine. The reaction mixture was stirred at room temperature for 12 h under nitrogen atmosphere and then it was treated with a 1:1 (v/v) water/methanol mixture to precipitate the product, which was filtered off. The resulting dark green solid was washed several times with methanol and acetone. The desired compound was obtained after drying in vacuo at 75 °C.

3.2.1. 2, 9 (10), 16 (17), 23 (24)-tetra-(2-pyridylethynyl) phthalocyaninatozinc (II) (3)

Yield: 53 mg (58%). ^{1}H NMR (500 MHz, [D6] DMSO): δ = 8.34–9.11 (m, 12H), 7.46–7.61 (m, 16H). UV/Vis [DMF, λ_{max} / nm (λ / logε)]: 357 (4.94), 681 (5.37). IR (FT-IR): υ_{max} = 3057, 1485, 1429, 1306, 1091. $C_{60}H_{28}N_{12}Zn$ (982.35): calcd. C 73.36; H 2.87; N 17.11 %; found: C 75.25; H 2.61; N 17.02 %. MALDI-TOF-MS: 982.13 $[M+2]^+$.

3.2.2. 2, 9 (10), 16 (17), 23 (24)-tetra-(2-pyridylethynyl) phthalocyaninatocobalt (II) (4)

Yield: 22 mg (24%). UV/Vis [DMF, λ_{max} / nm (λ / logε)]: 333 (4.91), 664 (5.01). IR (FT-IR): υ_{max} = 3060, 1439, 1392, 1309, 1098. $C_{60}H_{28}N_{12}Co$ (975.88): calcd. C 73.85; H 2.89; N 17.22 %; found: C 75.18; H 2.77; N 17.13 %. MALDI-TOF-MS: 1129.31$[M+DHB+2]^+$.

3.3. The general route for the synthesis of quaternized metallophthalocyanines (5, 6)

Compound **3** or **4** (100 mg, 0.14 mmol) was heated to 120 °C in DMF (5 mL) and excess dimethyl sulfate (0.1 mL) was added dropwise. The reaction mixture was stirred at 120 °C for 12 h. At the end of 12 h, the mixture was cooled to room temperature and the product was precipitated with acetone and collected by filtration. The green solid product was washed successively with hot ethanol, ethyl acetate, THF, chloroform, and diethyl ether.

3.3.1. Quaternized zincphthalocyanine (5)

Yield: 20 mg (16%). UV/Vis [DMF, λ_{max} / nm (λ / logε)]: 334 (4.46), 679 (4.74). IR (FT-TR): υ_{max} = 3055, 1512, 1207, 1095. $C_{64}H_{40}N_{12}O_8S_2Zn$ (1234.62): calcd. C 62.26; H 3.27; N 13.61 %; found: C 62.11; H 3.12; N 13.47 %.

3.3.2. Quaternized cobaltphthalocyanine (6)

Yield: 26 mg (21%). UV/Vis [DMF, λ_{max} / nm (λ / logε)]: 333 (5.38), 664 (5.42). IR (FT-TR): υ_{max} = 3065, 1440, 1395, 1310, 1095. $C_{64}H_{40}N_{12}O_8S_2Co$ (1228.14): calcd. C 62.59; H 3.28; N 13.69 %; found: C 62.39; H 3.22; N 13.51 %.

3.4. Determination of binding of Q-ZnPc and Q-CoPc to DNA using UV-Vis titrations

All titrations of Pcs with CT-DNA were performed at room temperature in the buffer solution. The concentrations of CT-DNA per nucleotide phosphate [DNA] was calculated from the absorbance at 260 nm using ε_{DNA} = 13200 M^{-1} cm^{-1}.[44] DNA was stored at 4 °C overnight and used within 2 days. Stock solutions of 20 μM quaternized Pcs (Q-ZnPc and Q-CoPc) and 50 μM DNA were prepared in buffer solution. First the absorption spectrum of 3 mL of buffer solution of Q-ZnPc and Q-CoPc was recorded and then 6 × 30 μL for Q-ZnPc (4 × 30 μL for Q-CoPc) injections of DNA were manually added. Absorption spectra were collected from 500 nm to 800 nm. The titrations were carried out until the Pc's Q-bands remained at a fixed wavelength upon the successive additions of CT-DNA. To determine the binding constants K_{bZnPc} and K_{bCoPc}, Eq. (1) (Table 1) was used:[45]

$$[DNA]/(\mathcal{E}_a - \mathcal{E}_f) = [DNA]/(\mathcal{E}_b - \mathcal{E}_f) + 1/[K_b((\mathcal{E}_b - \mathcal{E}_f)], \quad (1)$$

where the apparent absorption coefficients $\mathcal{E}_a$, $\mathcal{E}_f$, and $\mathcal{E}_b$ correspond to A_{obsd}/[Pc], the extinction coefficient of the free Pc, and the extinction coefficient of the Pc when fully bound to DNA, respectively. In plots of [DNA]/($\mathcal{E}_a - \mathcal{E}_f$) versus [DNA], K_b is given by the ratio of the slope to the intercept.[46] The experiments were repeated three times (Figures 3–5).

3.5. Determination of the change in thermal denaturation profile of DNA

Melting temperatures were determined for CT-DNA (50 μM, 2.5 mL) and quaternized Pcs (Q-ZnPc and Q-CoPc; 25 μM, 0.3 mL) in buffer by heating from 20 to 90 °C at a rate of 0.6 °C/min and recording the UV absorbance at 260 nm every 10 s (Figure 6). The absorbance measurements were repeated five times and standard deviations were calculated.[47]

3.6. Determination of thermodynamic parameters

The equilibrium constants of DNA:Pc complexes were determined by analyzing the absorbance of Pc-DNA solutions at varying temperatures (293.15 K, 303.15 K, 313.15 K, 323.15 K, 333.15 K). For the reversible binding reaction of a ligand that is binding to a DNA molecule with a single site to form a ligand–DNA complex, we can write the binding reaction as shown in Eq. (2):[48]

$$L + DNA \leftrightarrow LDNAK = [LDNA]_{eq}/([L]_{eq} \times [DNA]_{eq}), \tag{2}$$

where [L] is the concentration of the ligand or DNA-binding domain (in the present work, L represents Q-ZnPc and Q-CoPc), and $[DNA]_{eq}$ and $[LDNA]_{eq}$ are the concentrations of DNA and bound complex at equilibrium, respectively. The stability of the bound complex is determined by the differences in the noncovalent interactions between the Pc and the DNA as temperatures varied using a nonlinear least-squares algorithm.[48] At these temperatures, DNA does not undergo any structural degradation. The absorption spectra were analyzed by assuming phthalocyanine:DNA molar ratios as 1:1 and 2:1. The results show that the best fitting corresponds to the 1:1 model complex at studied temperatures. The energetics of DNA–phthalocyanine equilibrium can be conveniently characterized by three thermodynamic parameters: standard Gibbs free energy, ΔG°; standard molar enthalpy, ΔH°; and standard molar entropy, ΔS°. ΔG° can be calculated from the equilibrium constant, K, using a familiar relationship:

$$\Delta G^\circ = -RTlnK, \tag{3}$$

in which R and T represent the gas constant and the absolute temperature, respectively (Table 1).[24]

The van't Hoff equation (Eq. (4)) gives a linear plot of lnK versus 1/T (Figure 7) if the heat capacity change for the reaction is essentially zero:

$$dlnK/d(1/T) = -\Delta H^\circ/R. \tag{4}$$

ΔH° can be calculated from the slope of the straight line, $-\Delta H^\circ/R$, and the standard entropy by Eq. (5):

$$\Delta S^\circ = (\Delta H^\circ - \Delta G^\circ)/T, \tag{5}$$

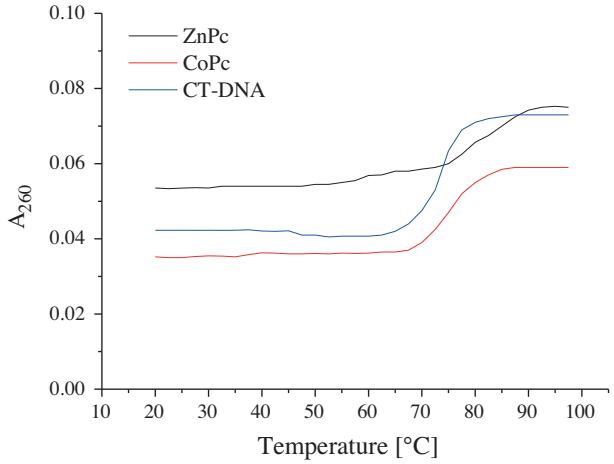

Figure 7. The thermal denaturation profiles of CT-DNA in the presence of Q-ZnPc and Q-CoPc.

Acknowledgment

This work was supported by the research funds of İstanbul Technical University.

References

1. McKeown, N. B. *Phthalocyanine Materials: Synthesis, Structure and Function.* Cambridge University Press: Cambridge, UK, 1998.
2. Thomas, A. L. *Phthalocyanine Research and Applications.* CRC Press: Boca Raton, FL, USA, 1990.
3. Rydosz, A.; Maciak, E.; Wincza, K.; Gruszczynski, S. *Sens. Actuators B Chem.* **2016**, *237*, 876-886.
4. Jeong, J.; Kumar, R. S.; Mergu, N.; Son, Y. A. *J. Mol. Struct.* **2017**, *1147*, 469-479.
5. Modlińska, A.; Chrzumnicka, E.; Martyński, T. *Opto-Electron. Rev.* **2017**, *25*, 296-302.
6. Poddutoori, P.; Poddutoori, P. K.; Maiya, B. G. *J. Porphyr. Phthalocya.* **2006**, *10*, 1-12.
7. Fiel, R. J.; Howard, J. C.; Mark, E. H.; Dattagupta, N. *Nucleic Acids Res.* **1979**, *6*, 3093-3118.
8. Duan, W.; Wang, Z.; Cook, M. J. *J. Porphyr. Phthalocya.* **2009**, *13*, 1255-1261.
9. Evren, D.; Burat, A. K.; Özçeşmeci, İ.; Sesalan, B. Ş. *Dyes Pigments* **2013**, *96*, 475-482.
10. Öztürk, R.; Kalay, Ş.; Kalkan, A.; Türkan, A.; Abasıyanık, M. F.; Bayır, Z. A.; Gül, A. *J. Porphyr. Phthalocya.* **2008**, *12*, 932-941.
11. Minicozzi, V.; Morante, S.; Rossi, G. C.; Stellato, F.; Christian, N.; Jansen, K. *Int. J. Quantum Chem.* **2008**, *108*, 1992-2015.
12. Rodriguez, M. E.; Fernandez, D. A.; Awruch, J.; Braslavsky, S. E.; Dicelio, L. E. *J. Porphyr. Phthalocya.* **2006**, *10*, 33-43.
13. Zhang, S.; Wang, J.; Zhao, Q.; Lu, X.; Zhou Q. *Structures and Interactions of Ionic Liquids.* Springer-Verlag: Berlin, Germany, 2014, pp. 39-77.
14. Gao, Y.; Sriram, M.; Wang, A. H. J. *Nucleic Acids Res.* **1993**, *21*, 4093-4101.
15. Özçeşmeci, İ.; Burat, A. K.; İpek, Y.; Koca, A.; Bayır, Z. A. *Electrochim. Acta* **2013**, *89*, 270-277.
16. Kalkan, A.; Koca, A.; Bayır, Z. A. *Polyhedron* **2004**, *23*, 3155-3162.
17. Özçeşmeci, İ.; Burat, A. K.; Bayır, Z. A. *J. Organomet. Chem.* **2014**, *750*, 125-131.
18. Sevim, A. M.; Yenilmez, H. Y.; Bayır, Z. A. *Polyhedron* **2013**, *62*, 120-125.
19. Yıldız, B. T.; Sezgin, T.; Çakar, Z. P.; Uslan, C.; Sesalan, B. Ş.; Gül, A. *Synth. Met.* **2011**, *161*, 1720-1724.
20. Evren, D.; Özçeşmeci, İ.; Sesalan, B. Ş.; Burat, A. K. *Synth. Met.* **2013**, *168*, 31-35.
21. Kurt, Ö.; Özçeşmeci, İ.; Sesalan B. Ş.; Koçak, M. B. *New J. Chem.* **2015**, *39*, 5767-5775.
22. Demirkapı, D.; Şirin, A.; Turanlı-Yıldız, B.; Çakar, Z. P.; Sesalan, B. Ş. *Synthetic Met.* **2014**, *187*, 152-159.
23. Dumoulin, F.; Durmuş, M.; Ahsen, V.; Nyokong, T. *Coord. Chem. Rev.* **2010**, *254*, 2792-2847.
24. Yenilmez, H. Y.; Sevim, A. M.; Bayır, Z. A. *Synthetic Met.* **2013**, *176*, 11-17.
25. Lapok L.; Claessens, C. G.; Wöhrle, D.; Torres, T. *Tetrahedron Lett.* **2009**, *50*, 2041-2044.
26. Sharman, W. M.; van Lier, J. E. *J. Porphyr. Phthalocya.* **2005**, *9*, 651-658.
27. Maya, E. M.; Haisch, P.; Vatzquez, P.; Torres, T. *Tetrahedron* **1998**, *54*, 4397-4404.
28. Özgür, N.; Nar, I.; Gül, A.; Hamuryudan, E. *J. Organomet. Chem.* **2015**, *781*, 53-58.
29. Karaoğlu, H. R. P.; Gül, A.; Koçak, M. B. *Dyes Pigments* **2008**, *76*, 231-235.

30. Kurt, Ö.; Koca, A.; Gül, A.; Koçak, M. B. *Synthetic Met.* **2015**, *206*, 72-83.

31. Turel, I.; Kljun, J. *Curr. Top. Med. Chem.* **2011**, *11*, 2661-2687.

32. Klug, A. *Q. Rev. Biophys.* **2010**, *43*, 1-21.

33. Anastassopoulou, J. *J. Mol. Struct.* **2003**, *651-653*, 19-26.

34. Rasouli, N.; Sohrabi, N. *Phys. Chem. Res.* **2016**, *4*, 83-94.

35. Yu, J. A.; Oh, S. H.; Park, Y. R.; Kim, J. S. *Macromol. Symp.* **2007**, *249-250*, 445-449.

36. Koçan, H.; Kaya, K.; Özçeşmeci, İ.; Sesalan, B. Ş.; Göksel, M.; Durmuş, M.; Burat, A. K. *J. Biol. Inorg. Chem.* **2017**, *22*, 1251-1266.

37. Indumathy, R.; Weyhermuller, T.; Nair, B. U. *Dalton Trans.* **2010**, *39*, 2087-2097.

38. Chairs, J. B. *Curr. Opin. Struc. Biol.* **1998**, *8*, 314-320.

39. Privalov, P. L.; Dragan, A. I.; Crane-Robinson, C. *Nucleic Acids Res.* **2011**, *39*, 2483-2491.

40. Louie, A. Y.; Meade, T. J. *P. Natl. Acad. Sci. USA* **1998**, *95*, 6663-6668.

41. Wartell, R. M.; Benight, A. S. *Phys. Reports* **1985**, *126*, 67-107.

42. Wolfe, A.; Shimer, G. H.; Meehan, T. *Biochemistry* **1987**, *26*, 6392-6396.

43. Sohrabi, N. *J. Pharm. Sci. Res.* **2015**, *7*, 533-537.

44. Turanlı-Yıldız, B.; Sezgin, T.; Çakar, Z. P.; Uslan, C.; Sesalan, B. Ş.; Gül, A. *Synthetic Met.* **2011**, *161*, 1720-1724.

45. Bayer, J.; Radler, J. O.; Blossey, R. *Nano Lett.* **2005**, *5*, 497-501.

46. Safaei, E.; Ranjbar, B.; Hasani, L. *J. Porphyr. Phthalocya.* **2007**, *11*, 805-814.

47. Thompson, M.; Woodbury, N. W. *Biochemistry* **2000**, *39*, 4327-4338.

48. Dezhampanah, H.; Darvishzad, T.; Aghazadeh, M. *Spectroscopy* **2011**, *26*, 357-365.